# Charge-Transfer Processes in Surface-Enhanced Raman Scattering. Franck–Condon Active Vibrations of Pyrazine

**ARTICLE** *in* THE JOURNAL OF PHYSICAL CHEMISTRY · FEBRUARY 1996

Impact Factor: 2.78 · DOI: 10.1021/jp952240k



**4 AUTHORS**, INCLUDING:

J. F. Arenas
University of Malaga
**107** PUBLICATIONS **1,571** CITATIONS
SEE PROFILE

Juan Carlos Otero
University of Malaga
**136** PUBLICATIONS **1,897** CITATIONS
SEE PROFILE

# Charge-Transfer Processes in Surface-Enhanced Raman Scattering. Franck−Condon Active Vibrations of Pyrazine

**Juan Francisco Arenas, Mark Steven Woolley, Juan Carlos Otero,* and Juan Ignacio Marcos**

*Department of Physical Chemistry, Faculty of Sciences, University of Málaga, E-29071 Málaga, Spain*

*Received: August 4, 1995; In Final Form: November 9, 1995*[⊗]

SERS spectra of pyrazine on silver electrode have been recorded and analyzed, assuming a charge transfer effect and using selection rules analogous to those of resonance Raman. With the aim of predicting the effect of this mechanism on the selective enhancement of fundamentals, a method has been proposed based on an analysis of the results of geometry optimizations carried out by ab initio calculations. The strongest SERS bands coincide with those assigned to the normal modes connecting the equilibrium geometries of the neutral molecule and the radical anion. These results support the presence of a charge transfer process from the metal to the adsorbate in the SERS spectra of pyrazine where a significant enhancement of vibrations 8a, 9a, 1, and 6a can be observed. The prediction capability of the analysis proposed here has been checked with published resonance Raman spectra of pyrazine and pyrazine-$d_4$. In all of the cases the strongest bands in the spectra are directly related to the largest $\Delta Q$ values obtained through the transformation $\Delta Q = L^{-1}\Delta R$.

## Introduction

Twenty years after the discovery of surface enhanced Raman scattering (SERS),[1,2] there now exists a general agreement that the enormous observed enhancement of the Raman signal is due mainly to two mechanisms, the electromagnetic (EM) and the charge transfer (CT) or chemical effect.[3−5] The selection rules derived from the EM mechanism are simple to apply as they resemble those of surface infrared spectroscopy and have been widely used. However, well defined selection rules that are capable of at least detecting the presence of the CT mechanism are not available given that this mechanism depends on the electronic structure of the particular metal−adsorbate system.

Some of the published SERS results for the pyrazine molecule are a good example of this.[6−9] In some works, a marked enhancement of the bands belonging to totally symmetric vibrations is seen that have been analyzed on the basis of the surface orientation of the adsorbate. However, similar results observed in the SERS of pyridine at sufficiently negative eletrode potentials have been satisfactorily explained assuming the existence of a charge transfer state accessible to the system under the experimental conditions.[4,10,11]

In general there are no simple rules that allow the recognition of which mechanism or mechanisms have given rise to a particular spectrum and therefore which class of selection rules should be applied. This puts in serious doubt the type of information that can be extracted from a SERS experiment: the surface orientation of the adsorbate (EM) or the properties of the electronic states involved in the charge transfer process (CT). In this respect, electron transmission and electron energy loss (EELS) experiments under resonance conditions (shape resonances[11−15]) have been quite useful in explaining the SERS-CT results. If the charge transfer in SERS-CT amounts to a complete electron, the transient state would correspond to the radical anion in both cases.[4] This parallelism has allowed Otto et al. to explain the SERS results of benzene on cold deposited silver or sodium,[4,16] as the most intense bands coincide essentially with those observed in electron impact experiments.[17] The selective enhancement mechanism of these bands is similar in both cases. These active bands are closely related to the differences between the equilibrium geometries of the two states involved;[18] the ground electronic state of the neutral molecule and that of the radical anion or the CT state in EELS or SERS, respectively. When the charge is trapped by the molecule, the nuclear structure relaxes in the direction of the potential energy surface minimum of the excited state. When the molecule comes back to its ground state, the normal modes connecting the equilibrium structures of the upper and the lower states remain excited much more probably than any other. Unfortunately, published works on shape resonances is rather scarce and the selection rules that have been proposed based on symmetry considerations are restricted to benzene.[15,19]

The origin of the selective enhancement of fundamentals that has been described is analogous to that of resonance Raman (RR) spectroscopy via Franck−Condon factors (*A* term).[20] In practice, the derived selection rules of this mechanism can be summarized by the well-known empirical rule of Tsuboi:[21] *if a Raman line becomes stronger when the excited frequency is brought into resonance with an electronic band, the equilibrium conformation of the molecule will be distorted along the normal coordinate of the given Raman line in the transition from the ground to the excited electronic state.* In a SERS-CT experiment, the situation is somewhat more complicated since the radical anion or the charge transfer states of a molecule such as pyrazine are not as well-known as are the excited singlets relevant in RR spectroscopy.

In this work we propose the use of geometry optimization results carried out by using ab initio calculations in order to detect the presence or absence of the CT mechanism in SERS. For this, we have assumed the hypothesis that in a SERS-CT experiment, an electron is transferred from the metal to the adsorbate, for which the CT state is equivalent to that of the radical anion from the molecular point of view. Since this chemical species is a doublet in its electronic ground state it will be named as the $D_0$ state. The analysis will consist of comparing the equilibrium geometries of the $S_0$ and the $D_0$ states in order to find out which portion of the molecule is the actual chromophore. In small aromatic molecules such as pyrazine the chromophore extends over its whole structure and as such the transferred electron density will be delocalized throughout

[⊗] Abstract published in *Advance ACS Abstracts,* January 15, 1996.

0022-3654/96/20100-3199$12.00/0 

the whole ring. Therefore, the chromophore will be characterized by means of those normal vibrations that connect the potential energy surface minimums. These vibrations will be active in SERS via a mechanism analogous to the A-term in RR spectroscopy. If in the obtained spectra an agreement between the observed enhancement and the theoretical prediction is observed, we will be in a position to confirm the presence of the CT mechanism and to extract information related to the charge transfer process giving rise to the spectra. As this is the first piece of work of this kind, a comparative discussion has been included employing several levels of calculation. The small size and the high symmetry of the pyrazine molecule has allowed this comparative study. Finally, a similar discussion applied to RR spectroscopy has also been included in order to check the validity of the process.

## Experimental Section

The chemical reagents used came from Aldrich and were of the highest available purity. Water was first deionized, triply distilled, and then degassified before being used in recording the SERS. Pyrazine was purified at reduced pressure in a Büchi GKR-51 distillator. Raman spectra were recorded in the 4000−100 $cm^{-1}$ range with a Jobin-Yvon U-1000 spectrometer fitted with a cooled Hamamatsu PMT 943−03 photomultiplier, using the 514.5 nm exciting line from a Spectra Physics 2020 $Ar^+$ laser with an effective power of 30 mW reaching the SERS sample. The spectra were recorded on a pure silver electrode (Metales Preciosos S.A.) that had been previously polished with 1.00, 0.30, and 0.05 $\mu$m alumina (Buehler). The working electrode was mounted in an electrochemical cell with a platinum counter electrode and a saturated Ag/AgCl reference electrode (Princeton Applied Research, PAR), to which all electrode potentials are referenced. A PAR Model 173 potentiostat and a PAR Model 175 programmer was used to control the electrode potentials. The electrode surface was electrochemically roughened in a 1 M aqueous solution of KCl by initially maintaining the surface potential at −0.50 V and then subjecting it to 10 2-s pulses at +0.60 V. Finally the SERS have been obtained from an aqueous solution of 0.1 M pyrazine and 1.0 M KCl at several surface potentials.

## Calculations

All of the geometry optimizations have been carried out by using the GAUSSIAN 90 package of programs[22] at diverse theoretical levels. For the ground-state RHF calculations were carried out employing different basis set functions, from 3-21G to 6-311++G*. For the radical anion UHF calculations have been carried out using the same basis set functions. Despite the fact that the spin contamination found in these results is moderate (in the order of 0.80−0.85 for all calculations) ROHF/3-21G and 3 × 3 UNO-CAS/3-21G, 6-31+G and 6-31++G calculations were also carried out since these methods have already proved to be adequate in studying radicals.[23,24] For this last method, all UHF natural orbitals with occupation numbers between 1.98 and 0.02 have been included in the active space according to the criteria of Pulay et al.[25] The geometries of the first two excited states of pyrazine of $^1B_{3u}$ ($S_1$) and $^1B_{2u}$ ($S_2$) symmetry have been optimized by means of CIS/3-21G calculations.

Although the direct comparison between the optimized geometric parameters of the $S_0$ and $D_0$ (or $S_i$) states gives valid information in determining the Franck−Condon active vibrations in SERS-CT or RR, we propose here the use of a simple numerical treatment that is often used in electronic spectroscopy.[26,27] It is based on the well known transformation in vibrational spectroscopy between the internal coordinates (**R**) and the normal modes of vibration (**Q**) via the **L** matrix:

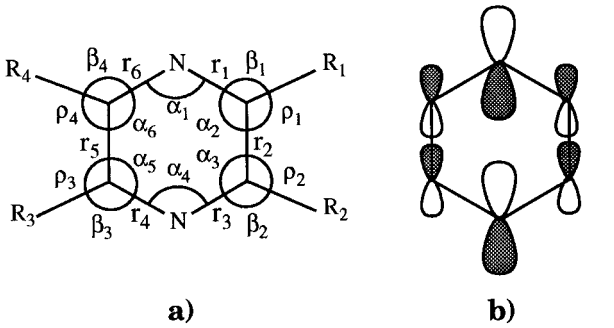


**Figure 1.** In-plane internal coordinates (a) and pictorial representation of the LUMO ($B_{3u}$) of pyrazine (b).

$$\mathbf{R} = \mathbf{LQ} \tag{1}$$

Using the transformation

$$\Delta\mathbf{Q} = \mathbf{L}^{-1}\Delta\mathbf{R} \tag{2}$$

it is possible to determine $\Delta\mathbf{Q}$ which is a vector that vibrationally characterizes the chromophore and represents the displacement of the potential energy surface minimums of the two states implicated in the resonance process along each normal coordinate. $\Delta\mathbf{R}$ is a vector that contains the differences between the geometric parameters of the excited states ($D_0$ in SERS-CT or $S_i$ in RR) and the ground state ($S_0$) and will be built from the results of the optimized geometries. The L matrix of the ground electronic state needs to be known for which the force field at RHF/3-21G level has been calculated. These $\Delta\mathbf{Q}$ amplitudes can be used afterward to calculate excitation profiles in SERS-CT or RR[20] spectra or in deducing active Franck−Condon vibrations in absorption.[26] In the case of pyrazine the vector $\Delta\mathbf{Q}$ will contain exclusively totally symmetric vibrations since all of the here studied equilibrium structures belong to the $D_{2h}$ point group.

## Results and Discussion

**Raman Spectra of Pyrazine in Its Electronic Ground State.** The vibrational spectrum of pyrazine has been studied by ourselves, among others.[28,29] The five fundamental vibrations of $A_g$ symmetry for the pure liquid are recorded at 3055, 1580, 1233, 1016, and 602 $cm^{-1}$ and are assigned to the modes 2;$\nu$(CH), 8a;$\nu_{ring}$, 9a;$\delta$(CH), 1;$\nu_{ring}$ and 6a;$\delta_{ring}$, respectively, according to Wilson's nomenclature.[30] The L matrix for the in-plane vibrations has been built starting with the ab initio force field and following a process analogous to that described elsewhere.[31] First, the internal coordinates have been defined as shown in Figure 1a, and then linear combinations have been defined according to the recommendations of Pulay et al.[32] (Table 1). The ab initio **F** matrix in Cartesian coordinates has been transformed into independent internal coordinates by using the program FLINT,[29] and afterward a modified version of the program QCPE#576[33] was used to carry out the normal-coordinate analysis. This version also permits the application of the scaled quantum mechanical methodology of Pulay et al.[34] in order to correct for the systematic errors of the ab initio methods. The scaling process was carried out by adjusting the 17 in-plane frequencies of the pure liquid of the normal isotopomer. It was necessary to optimize only two scale factors that affect the diagonal elements of the **F** matrix and an extra factor for the $\nu$(CC) interactions in ortho, meta, and para positions as is the case with benzene.[31] The numerical values

**TABLE 1: In-Plane Internal Coordinates and Refined Scale Factors**

| character | internal coordinate | | scale factor |
|---|---|---|---|
| $\nu$(C−H) | $\mathbf{R_{1-4}} = R_i$ | $i = 1-4$ | 0.80 |
| $\nu_{ring}$ | $\mathbf{R_{5-10}} = r_i$ | $i = 1-6$ | 0.86 |
| $\delta$(C−H) | $\mathbf{R_{11-14}} = 2^{-1/2}(\beta_i - r_i)$ | $i = 1-4$ | 0.80 |
| $\delta_{ring}$ | $\mathbf{R_{15}} = 6^{-1/2}(\alpha_1 - \alpha_2 + \alpha_3 - \alpha_4 + \alpha_5 - \alpha_6)$ | | 0.80 |
| | $\mathbf{R_{16}} = 12^{-1/2}(2\alpha_1 - \alpha_2 - \alpha_3 + 2\alpha_4 - \alpha_5 - \alpha_6)$ | | |
| | $\mathbf{R_{17}} = 4^{-1/2}(-\alpha_2 + \alpha_3 - \alpha_5 + \alpha_6)$ | | |
| $\nu_{ring}$ coupling in ortho, meta, and para positions | | | 0.76 |

**TABLE 2: Frequencies ($cm^{-1}$) of In-Plane $A_g$ Fundamentals of Pyrazine**

| mode | $\nu_{obs}$ | $\nu_{calc}$/ 3-21G | $\nu_{calc}$/ 6-31+G*[a] | $\nu_{scaled}$ | PED (%) |
|---|---|---|---|---|---|
| 2;$\nu$(CH) | 3055 | 3418 | 3402 | 3057 | 100 $\nu$(CH) |
| 8a;$\nu_{ring}$ | 1580 | 1732 | 1798 | 1585 | 68 $\nu_{ring}$; 24 $\delta$(CH) |
| 9a;$\delta$(CH) | 1233 | 1362 | 1358 | 1232 | 72 $\delta$(CH); 26 $\nu_{ring}$ |
| 1;$\nu_{ring}$ | 1016 | 1111 | 1125 | 1015 | 96 $\nu_{ring}$ |
| 6a;$\delta_{ring}$ | 602 | 678 | 654 | 607 | 90 $\delta_{ring}$ (**$R_{16}$**) |

[a] Taken from ref 35.

of the final scale factors, the scaled and 3-21G calculated frequencies, and the PED of each normal mode can be seen in Tables 1 and 2. 6-31+G* calculated frequencies taken from ref 35 have been included also in Table 2 in order to show that the basis set does not significantly affect this type of result. The only feature to point out in the PED is the significant contribution of the $\nu_{ring}$ coordinates in the description of the 9a mode.

The relative intensities of the Raman bands of the pure liquid and aqueous solution can be seen in Table 3. All of the relative intensities have been normalized against the 1 vibration which has been arbitrarily assigned the value of 100. Generally speaking, the strongest Raman lines correspond to $A_g$ modes, with the exception of the vibration 4;$\gamma_{ring}$,$B_{2g}$which is the most intense of those remaining, with a normalized intensity of 5.

**SERS Results.** The relative SERS intensities of the $A_g$ fundamentals for pyrazine reported in previous works are collected in Table 3. As can be seen, the relative intensities of the SERS on silver sol from Sbrana et al.[6] do not change significantly with respect to those obtained by conventional Raman spectroscopy. The most notable difference is the reduction in intensity of the $\nu$(CH) band or the increase in intensity of the 8a which is found to be multiplied by a factor close to 2. The spectrum obtained by Moskovits et al. in a gas−solid interface at submonolayer coverage has similar characteristics to that of the pure liquid or the colloid, with the only bands rising above the background corresponding to the 1 and the 8a modes.[9] This same spectrum obtained at a higher surface coverage, at approximately one monolayer, shows a considerable increase in the relative intensities of the bands corresponding to the 6a, 9a, and 8a modes.[9] These authors explain this result in terms of the EM mechanism selection rules proposing a change in the surface orientation induced by the coverage. The molecule changes from a *face-on* to an *end-on* orientation, thus accommodating more molecules on the surface. The fact is that Sbrana et al. analyze their results in colloid also employing the same type of selection rules, proposing an *end-on* orientation from a spectra of intensity characteristics that are quite apart from those of Moskovits et al. at high coverage. The SERS spectra on electrode included in Table 3 show characteristics similar to those of Moskovits et al. at high coverage, especially in the result from Erdheim et al.[8] obtained at −0.4 V vs SCE. That work centers its interest on the observation of forbidden bands and does not arrive at any conclusion concerning the surface orientation. Our own results in the electrode potential range of 0.00 to −0.75 V (Figure 2) have been summarized in Table 4. As can be seen, in every case there exists a noticeable enhancement of the $A_g$ vibrations with respect to the solution spectra in agreement with the aforementioned bibliographic results on an electrode and on a gas−solid interface at high concentration. It can be seen in Table 4 how the relative intensities of the bands with respect to that of the 1 mode reach a maximum in the spectra recorded at −0.25 and −0.50 V, the only exception being the 2;$\nu$(CH) mode, whose intensity decreases steadily on going to more negative electrode potentials. Upon comparing the spectra measured at 0.00 and −0.25 V, it can be seen that bands of the 8a, 9a, and 6a fundamentals increase in intensity by a factor of about 2 in all cases. When the electrode potential is made more negative the intensity of the 9a vibration reaches its maximum at −0.50 V, with that of the 6a losing intensity much more slowly than the 8a.

The SERS spectra of pyridine obtained at negative potentials is one of the few examples where the CT mechanism has been verified. Given that these spectra show a systematic enhancement of the bands due to the 6a, 9a, and 8a modes,[11] it would be reasonable to expect that an analogous mechanism would operate in a molecule with a similar electronic structure such as pyrazine. This possibility is also supported by several facts: (a) as in pyridine, CT bands in EELS,[36] and visible[37] spectra are observed for the silver−pyrazine system for a range of energies accessible with visible photons usually used in a conventional Raman experiment (2−2.5 eV);[38] (b) the LUMO (orbital accepting the transferred charge) is more stable in pyrazine than in pyridine, resulting in the electron affinity for pyrazine in the gas phase being positive while that for pyridine is negative;[14] (c) the energy difference between the $S_0$ and the $D_0$ states is less for pyrazine than it is for pyridine (1.37 and 2.22 eV respectively from RHF/3-21G and UHF/3-21G results). These considerations are in agreement with the different behavior of the SERS of both molecules. In the case of pyrazine the band due to the 8a mode is visible even at 0.00 V with a relative intensity of 72 (Table 4), while for pyridine it is necessary to go to much more negative potentials in order to observe a similar enhancement of this mode.[11] All of these facts indicate that the CT state in pyrazine should be considerably more accessible than in pyridine, and as such there is the possibility that the enhancement of the 6a, 9a, and 8a modes in some of the spectra summarized in Tables 3 and 4 occurs via the CT mechanism. The relative enhancement of these fundamentals to a level comparable to that of the vibration 1 is seen in the whole series of SERS results of pyrazine on silver electrode. The spectra that show these characteristics, like those of Birke et al. and Moskovits et al. at high coverage, and those of this work will subsequently be referred to as SERS-CT. As can be seen, the relative intensities of these bands recorded in SERS on electrode vary from author to author, but a noticeable enhancement is observed in every case. In this respect it has to be pointed out that the relative intensity is not only a function of the electrode potential and the photon energy but also of the preparation method of the surface which often differs from work to work.

The bond lengths and angles corresponding to the $S_0$ ($^1A_{1g}$) and $D_0$ ($^2B_{3u}$) optimized geometries calculated using several theoretical levels are shown in Table 5. In every case, the difference between the HCN ($\beta$) and HCC ($\rho$) bond angles has been included, given that the internal coordinates $\delta$(CH) are

**TABLE 3: Summary of the Relative Intensities of $A_g$ Fundamentals in Raman, SERS, and Resonance Raman Spectra of Pyrazine[a]**

| | Raman | | SERS | | | | | resonance Raman | | |
|---|---|---|---|---|---|---|---|---|---|---|
| mode | liquid | solution | sol | electrode | electrode | monolayer | submonolayer | $S_0-S_1$ | $S_0-S_2$ | $S_0-(S_2-d_4)$ |
| 2 | 17 | 17 | 7 | 25 | | | | | | |
| 8a | 7 | 9 | 13 | 107 | 67 | 83 | 14 | 44 | | |
| 9a | 6 | 7 | 8 | 18 | 53 | 22 | | 222 | | 20 |
| 1 | 100 | 100 | 100 | 100 | 100 | 100 | 100 | 100 | 100 | 100 |
| 6a | <1 | <1 | 1 | 31 | 5 | 34 | | 78 | 100 | 100 |
| 4b | 5 | 1 | | | | | | | | |
| ref | | | 6 | 8 | 7 | 9 | 9 | 39 | 39 | 39 |

[a] The intensities are measured as the height of the bands. The band intensity of the vibration 1 arbitrarily equal to 100. [b] Data for vibration 4;$\gamma_{ring}$,$B_{2g}$ are included for comparison.

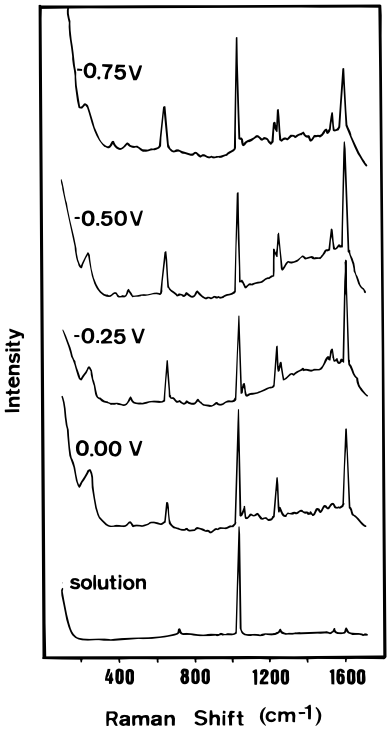


**Figure 2.** Raman spectra of the aqueous solution and SERS on silver electrode of pyrazine.

**TABLE 4: Relative Intensities of $A_g$ Fundamentals Measured in the SERS of Pyrazine (Electrode Potentials Measured vs Ag/AgCl Saturated Electrode)**

| mode | 0.00 V | −0.25 V | −0.50 V | −0.75 V |
|---|---|---|---|---|
| 2 | 19 | 16 | 12 | 7 |
| 8a | 72 | 131 | 113 | 49 |
| 9a | 10 | 25 | 37 | 28 |
| 1 | 100 | 100 | 100 | 100 |
| 6a | 21 | 48 | 48 | 36 |
| 4[a] | 2 | 7 | 9 | |

[a] Data for vibration 4;$\gamma_{ring}$,$B_{2g}$ are included for comparison.

defined in this way (see Table 1). The lower part of Table 5 shows the differences between the equilibrium structures and the energies of the two states. The extra electron produces a similar effect to that in benzene with respect to its radical anion in the $^2B_{3u}$ state.[23] The C−C bond lengths ($r_{2,5}$) shorten while those of the C−N ($r_{1,3,4,6}$) lengthen as could be expected in view of the molecular orbital acceptor of the charge (LUMO, $B_{3u}$; Figure 1b). As can be seen in Table 5, no theoretical level is able to reproduce the experimental result that the radical anion is more stable than the neutral molecule,[14] given that all of the results for $\Delta E$ are positive. As the size of the basis set increases the anion is found to be more stable (1.37 and 0.66 eV with 3-21G and 6-311++G basis set, respectively). When polarization functions are included, then an increase of some 20% is computed (0.78 eV with 6-311++G* for instance). If the energies of the $D_0$ state are computed via MCSCF calculations, the respective $\Delta E$ values are reduced by some 50% (0.78 and 0.34 eV at 3 × 3 UNO-CAS/3-21G and 6-31++G level respectively).

The $\Delta E$ values are found to be much more sensitive to the level of theory than are the geometries. From the differences between the geometries of the $S_0$ and $D_0$ states it comes out that a molecular deformation similar to that qualitatively represented in Figure 3a is always predicted, irrespective of the theoretical level. As can be appreciated the structure of the $D_0$ state is affected very little by the type of calculation used, with practically identical geometries for UHF, ROHF, and UNO-CAS with 3-21G basis set. This is due to the moderate amount of spin contamination in the UHF calculations and the small degree of nondynamical correlation detected that does not require an active space greater than 3 × 3. On the contrary, the size of the basis set does produce more important effects. Although it is generally accepted that the electronic representation of anionic species requires the use of diffuse basis set functions, it can be seen that the 6-31+G or 6-31++G results do not differ significantly from those of 6-31G. However, the addition of polarization functions does affect the geometries of both states. Generally speaking, upon increasing the basis set size the magnitude of the molecular distortion decreases, although the behavior is reasonably systematic, in such a way that 3-21-G results overestimate by approximately 20% those obtained by using 6-31+G* or 6-311++G*; the only exception being $\Delta\delta$(CH) coordinates where the sign is inverted.

A qualitative prediction of the modes which will be active in either SERS-CT or EELS under resonant conditions can be deduced from Figure 3a by inspection. It can be seen that the differences for the bond stretchings are much greater for the ring bonds than for the CH ones, given that the electron is essentially located in the aromatic skeleton. Therefore, the contribution of the $\nu$(CH) vibration to the chromophore will be small in agreement with the relative intensities of the SERS-CT spectra. The ring bonds are distorted in a way similar to that of the 8a mode ($r_{1-6}$: +−++−+), accounting for the activity of this vibration. A similar behavior is observed for bendings, the most marked difference being in the ring angles rather than in the $\Delta\delta$(CH). In this last case it is important not to forget that the PED of the 9a mode contains an important $\nu_{ring}$ contribution. The ring deformation has a similar form to that of the internal coordinate $R_{16}$ that contributes 90% to the PED of the 6a vibration at 602 $cm^{-1}$. Despite the fact that the SERS-CT or RR intensities are related to these geometric differences via complicated mathematical equations,[20] it becomes clear that a simple comparison of the equilibrium structures of the two states can explain, at least qualitatively, the observed behavior in the spectra.

**TABLE 5: Optimized Equilibrium Structures of the Ground State ($S_0$), the Radical Anion ($D_0$), and the Two Lowest Singlet Excited States ($S_1$,$S_2$) of Pyrazine (Bond Lengths in angstroms and Angles in Degrees)[a]**

| basis set: | 3-21G | | | 6-31G | 6-31+G | | 6-31+G* | 6-31++G | | 6-311++G | 6-311++G* | 3-21G | 3-21G |
|---|---|---|---|---|---|---|---|---|---|---|---|---|---|
| state | $S_0$: | | | | | | | | | | | $S_0$: | $S_0$: |
| method: | RHF | RHF | RHF | RHF | RHF | RHF | RHF | RHF | RHF | RHF | RHF | RHF | RHF |
| parameter: | | | | | | | | | | | | | |
| $r_{1,3,4,6}$ | 1.3310 | 1.3310 | 1.3310 | 1.3317 | 1.3322 | 1.3322 | 1.3192 | 1.3323 | 1.3323 | 1.3315 | 1.3172 | 1.3310 | 1.3310 |
| $r_{2,5}$ | 1.3808 | 1.3810 | 1.3808 | 1.3857 | 1.3871 | 1.3871 | 1.3879 | 1.3871 | 1.3871 | 1.3848 | 1.3863 | 1.3808 | 1.3808 |
| $R$ | 1.0687 | 1.0687 | 1.0687 | 1.0690 | 1.0690 | 1.0690 | 1.0746 | 1.0691 | 1.0691 | 1.0675 | 1.0750 | 1.0687 | 1.0687 |
| $\alpha_{2,3,5,6}$ | 120.99 | 120.99 | 120.99 | 120.95 | 120.99 | 120.99 | 121.69 | 120.98 | 120.98 | 121.04 | 121.69 | 120.99 | 120.99 |
| $\alpha_{1,4}$ | 118.01 | 118.01 | 118.01 | 118.09 | 118.03 | 118.03 | 116.62 | 118.04 | 118.04 | 117.92 | 116.61 | 118.01 | 118.01 |
| $\beta_{1-4}$ | 117.69 | 117.69 | 117.69 | 117.34 | 117.27 | 117.27 | 117.38 | 117.26 | 117.26 | 117.30 | 117.41 | 117.69 | 117.69 |
| $\rho_{1-4}$ | 121.32 | 121.32 | 121.32 | 121.71 | 121.74 | 121.74 | 120.93 | 121.76 | 121.76 | 121.66 | 120.90 | 121.32 | 121.32 |
| $\delta$CH: $(\beta-\rho)_{1-4}$ | −3.63 | −3.63 | −3.63 | −4.37 | −4.47 | −4.47 | −3.55 | −4.50 | −4.50 | −4.36 | −3.49 | −3.63 | −3.63 |
| state | $D_0$: | | | | | | | | | | | $S_1$: | $S_2$: |
| method: | UHF | ROHF | CAS[c] | UHF | UHF | CAS[c] | UHF | UHF | CAS[c] | UHF | UHF | CIS | CIS |
| parameter: | | | | | | | | | | | | | |
| $r_{1,3,4,6}$ | 1.3887 | 1.3823 | 1.3916 | 1.3836 | 1.3830 | 1.3863 | 1.3664 | 1.3831 | 1.3863 | 1.3832 | 1.3649 | 1.3427 | 1.3648 |
| $r_{2,5}$ | 1.3528 | 1.3536 | 1.3525 | 1.3594 | 1.3644 | 1.3633 | 1.3644 | 1.3644 | 1.3633 | 1.3616 | 1.3625 | 1.3862 | 1.4117 |
| $R$ | 1.0771 | 1.0772 | 1.0770 | 1.0767 | 1.0746 | 1.0747 | 1.0800 | 1.0747 | 1.0748 | 1.0735 | 1.0806 | 1.0687 | 1.0692 |
| $\alpha_{2,3,5,6}$ | 124.36 | 124.14 | 124.53 | 124.04 | 123.74 | 123.93 | 124.46 | 123.74 | 123.93 | 123.83 | 124.46 | 119.45 | 123.58 |
| $\alpha_{1,4}$ | 111.28 | 111.72 | 110.94 | 111.92 | 112.52 | 112.14 | 111.08 | 112.52 | 112.13 | 112.33 | 111.08 | 121.10 | 112.84 |
| $\beta_{1-4}$ | 115.89 | 116.05 | 115.78 | 115.81 | 115.85 | 115.74 | 116.20 | 115.84 | 115.74 | 115.90 | 116.29 | 120.69 | 116.90 |
| $\rho_{1-4}$ | 119.75 | 119.81 | 119.69 | 120.15 | 120.41 | 120.33 | 119.34 | 120.41 | 120.33 | 120.27 | 119.25 | 119.86 | 119.52 |
| $\delta$CH: $(\beta-\rho)_{1-4}$ | −3.86 | −3.76 | −3.91 | −4.34 | −4.56 | −4.59 | −3.14 | −4.65 | −4.59 | −4.37 | −2.96 | 0.83 | −2.62 |
| diff | $\Delta(D_0 - S_0)$: | | | | | | | | | | | $(S_1 - S_0)$: | $(S_2 - S_0)$: |
| $\Delta r_{1,3,4,6}$ | 0.0577 | 0.0513 | 0.0606 | 0.0519 | 0.0508 | 0.0541 | 0.0472 | 0.0508 | 0.0540 | 0.0417 | 0.0477 | 0.0117 | 0.0338 |
| $\Delta r_{2,5}$ | −0.028 | −0.0272 | −0.0283 | −0.0263 | −0.0227 | −0.0238 | −0.0235 | −0.0227 | −0.0238 | −0.0232 | −0.0238 | 0.0054 | 0.0309 |
| $\Delta R$ | 0.0084 | 0.0085 | 0.0083 | 0.0077 | 0.0056 | 0.0057 | 0.0054 | 0.0056 | 0.0057 | 0.0060 | 0.0056 | 0.0000 | 0.0005 |
| $\Delta\alpha_{2,3,5,6}$ | 3.37 | 3.15 | 3.54 | 3.09 | 2.75 | 2.94 | 2.77 | 2.76 | 2.95 | 2.79 | 2.77 | −1.54 | 2.59 |
| $\Delta\alpha_{1,4}$ | −6.73 | −6.29 | −7.07 | −6.17 | −5.51 | −5.89 | −5.54 | −5.52 | −5.91 | −5.59 | −5.33 | 3.08 | −5.17 |
| $\Delta\beta_{1-4}$ | −1.80 | −1.64 | −1.91 | −1.53 | −1.42 | −1.53 | −1.18 | −1.42 | −1.52 | −1.40 | −1.12 | 3.01 | −0.79 |
| $\Delta\rho_{1-4}$ | −1.57 | −1.51 | −1.63 | −1.56 | −1.33 | −1.42 | −1.59 | −1.35 | −1.43 | −1.39 | −1.65 | −1.46 | −1.80 |
| $\Delta\delta$CH | −0.23 | −0.13 | −0.28 | 0.03 | −0.09 | −0.12 | 0.42 | −0.15 | −0.09 | −0.01 | 0.53 | 4.47 | 1.01 |
| $\Delta$energy (eV):[b] | 1.37 | 1.78 | 0.78 | 1.11 | 0.67 | 0.34 | 0.81 | 0.67 | 0.34 | 0.66 | 0.78 | 4.81 | 6.57 |

[a] See Figure 1a and Table 1 for symbols. [b] Differences between the energies of $D_0$ or $S_i$ states and $S_0$. [c] 3 × 3 UNO-CAS.

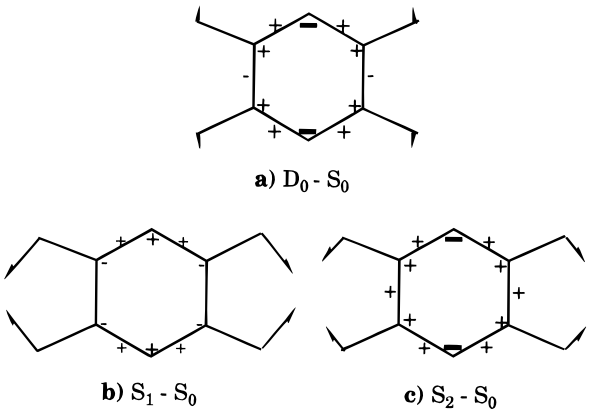


**Figure 3.** Qualitative in-plane changes between the geometries of the ground electronic state ($S_0$), the radical anion ($D_0$ (a)), and the two lowest excited states of pyrazine ($S_1$ (b) and $S_2$ (c)).

To carry out the transformation (2), a set of combinations of bond lengths (in angstroms) and angles (in radians) have been calculated, employing the same numerical expressions that were used in defining the internal coordinates (Table 1). In this way $\Delta\mathbf{R}$ and $\mathbf{L}^{-1}$ are compatible and the displacements along each normal coordinate $\Delta\mathbf{Q}$ can be extracted from the difference $\Delta\mathbf{R} = \mathbf{R}(D_0) - \mathbf{R}(S_0)$. The final $\Delta\mathbf{Q}$ value for a particular fundamental is the result of the sum or the difference of the contributions, depending on the sign of the vector components of $\Delta\mathbf{R}$ and the elements of the $\mathbf{L}^{-1}$ matrix, in such a way that it is possible that contributions due to different geometric parameters cancel each other either partially or completely for some of the fundamentals.

Table 6 shows the values of $\Delta\mathbf{Q}$ obtained using diverse levels of theory by means of the scaled $\mathbf{L}^{-1}$ matrix. The influence of the calculation level on the values of $\Delta\mathbf{Q}$ is completely analogous to that previously discussed, and generally speaking, they decrease when the size of the basis set increases. Provided that the relative intensities of the SERS bands depend on the relative values of $\Delta\mathbf{Q}$, the most important conclusion is that the level of theory does not significantly affect the analysis of the spectra. When the $\Delta\mathbf{Q}$ value is normalized to 100 for vibration 1, then the values for 8a, 9a, and 6a fundamentals are found to be either 91, 77, and 162, respectively, or 93, 86, and 168 when 3-21G and 6-31+G* basis set are used, respectively. It comes out clearly that the differences are negligible when one compares them with the relative intensities reported by different authors in similar SERS (see Tables 3 and 4).

The 6-31+G* value of $\Delta\mathbf{Q}$ for the 9a vibration exhibits the same sign as the other columns despite that in this case $\Delta\delta(CH) > 0$. This is due to the value of −0.141 being obtained essentially from the ring stretching contributions. A column showing the results of the transformation using the calculated $\mathbf{L}^{-1}$ matrix has also been included, being very similar to those of the scaled results. As can be appreciated the values of $\Delta\mathbf{Q}$ for all of the fundamentals with $A_g$ symmetry are comparable, with the exception of the 2 mode. The 1, 9a, and 8a vibrations have very similar values while, that of the 6a has a significantly higher value. It can be seen that these values of $\Delta\mathbf{Q}$ are not directly proportional to the SERS-CT intensities of these modes, but they do reproduce fairly well the experimental behavior, keeping in mind that the largest $\Delta\mathbf{Q}$ value corresponds to a Raman band that has a relative intensity of less than 1 in the

**TABLE 6: Normal-Mode Displacement (ΔQ) between the Equilibrium Structures of the Ground State ($S_0$) and That of the Anion ($D_0$) and the Two Lowest Singlet Excited States of Pyrazine ($S_1$ and $S_2$)**

| basis set: | | 3-21G | | | | 6-31G | 6-31+G | | 6-31+G* | 6-31++G | | 6-311++G | 6-311++G* | 3-21G | 3-21G | 3-21G |
|---|---|---|---|---|---|---|---|---|---|---|---|---|---|---|---|---|
| state | | $S_0$: | | | | | | | | | | | | $S_0$: | $S_0$: | |
| method: | | RHF | RHF | RHF | RHF | RHF | RHF | RHF | RHF | RHF | RHF | RHF | RHF | RHF | RHF | RHF |
| state | | $D_0$ | | | | | | | | | | | | $S_1$: | $S_2$: | |
| method: | | UHF | UHF | ROHF | CAS[a] | UHF | UHF | CAS[a] | UHF | UHF | CAS[a] | UHF | UHF | CIS | CIS | CIS |
| $L^{-1}$ ($S_0$) | | scaled | calc | scaled | scaled | scaled | scaled | scaled | scaled | scaled | scaled | scaled | scaled | scaled | scaled | scaled-$d_4$ |
| mode | $\nu$ | **ΔQ** | **ΔQ** | **ΔQ** | **ΔQ** | **ΔQ** | **ΔQ** | **ΔQ** | **ΔQ** | **ΔQ** | **ΔQ** | **ΔQ** | **ΔQ** | **ΔQ** | **ΔQ** | **ΔQ** |
| 2,$\nu$(CH) | 3055 | 0.016 | 0.016 | 0.017 | 0.016 | 0.015 | 0.010 | 0.011 | 0.010 | 0.010 | 0.011 | 0.011 | 0.010 | −0.005 | −0.003 | −0.012 |
| 8a,$\nu_{ring}$ | 1580 | −0.188 | −0.183 | −0.173 | −0.196 | −0.171 | −0.159 | −0.169 | −0.152 | −0.159 | −0.169 | −0.162 | −0.152 | 0.036 | −0.017 | −0.026 |
| 9a,$\delta$(CH) | 1233 | −0.158 | −0.172 | −0.143 | −0.164 | −0.147 | −0.141 | −0.149 | −0.141 | −0.141 | −0.149 | −0.146 | −0.144 | −0.123 | −0.030 | 0.128 |
| 1,$\nu_{ring}$ | 1016 | −0.206 | −0.197 | −0.174 | −0.219 | −0.181 | −0.189 | −0.202 | −0.164 | −0.189 | −0.202 | −0.192 | −0.166 | −0.092 | −0.244 | 0.236 |
| 6a,$\delta_{ring}$ | 602 | −0.333 | −0.332 | −0.312 | 0.352 | −0.305 | −0.270 | −0.270 | −0.275 | −0.271 | −0.291 | −0.273 | −0.274 | 0.192 | −0.390 | −0.376 |

[a] 3 × 3 UNO-CAS.

pure and aqueous solution Raman spectra. Two important differences can be extracted from **ΔQ** with respect to the conclusions obtained from a simple comparison between the geometries: (a) now it is possible to explain the SERS-CT activity of the 9a mode that was not evident in the previous discussion, showing a **ΔQ** amplitude comparable to the remaining vibrations; and (b) the 1 mode forms part of the chromophore. This last point is important since SERS intensities are often referenced to some ring breathing mode, which can lead to believing that it is not active via this mechanism. As can be seen, the SERS-CT band of this vibration does intensify with respect to others that are less active such as the $\nu$(CH).

**Resonance Raman Spectra.** The relative intensities of the Raman spectra of pyrazine near-resonant with the $S_1(^1A_{1g}-^1B_{3u})$ and resonant with the $S_2(^1A_{1g}-^1B_{2u})$ states showed in Table 3 have been taken from those reported by Suzuka et al.[39] The spectrum obtained in near-resonance with the first excited state is found to be dominated by the band assigned to the 10a;$\gamma$(CH),$B_{1g}$ mode given that it is responsible for the vibronic coupling between the two mentioned excited singlets ($B_{2u} \times B_{3u} = B_{1g}$). The strengthening of this non-totally-symmetric fundamental occurs via the *B* term in RR due to the Herzberg−Teller effect, such that the procedure we propose based on geometric changes cannot account for the activity of this fundamental. The remaining fundamentals in this spectrum have been assigned to totally symmetric modes, the most intense band being that assigned to vibration 9a. Table 5 shows also the geometric parameters of the CIS/3-21G optimized geometries of the $S_1$ and $S_2$ states. On comparing the $S_0$ and $S_1$ geometries it can be seen that, in general, the differences are less than those observed in the case of SERS-CT, with one exception: the value of $\Delta\delta$(CH), which is 4.47°, against differences smaller than 1° obtained previously. A qualitative view of the changes in the potential energy surface minimums can be seen in Figure 3b. The final **ΔQ** values obtained reflecting the same behavior (Table 6); those assigned to the 6a, 1, and 8a modes being significantly smaller than in SERS, while that for the 9a mode remains comparable, in agreement with the experimental results.

The spectrum upon exciting pyrazine to the second excited singlet shows quite different characteristics. Now only the 6a and 1 vibrations are active with similar intensities. For the transition $S_2-S_0$, the changes in geometry are similar to those obtained in SERS (Table 5) with the exception of the 8a mode which is now barely active, given that the changes in bond stretching behave essentially the same as in the 1 mode ($r_{1-6}$: ++++++) (see Figure 3c). The values of **ΔQ** in the column corresponding to the $S_2-S_0$ transition in Table 6 support correctly that the only observed fundamentals should be the 1 and the 6a.

In the work of Suzuka et al.[39] the RR study between the states $S_2-S_0$ of deuterated pyrazine has also been included. Compared to the normal isotopomer, the spectrum of the deuterated one shows three active fundamentals recorded at 1003, 886, and 581 $cm^{-1}$ for the pure liquid Raman of pyrazine-$d_4$ and are assigned to 9a, 1, and 6a vibrations.[28,39] In RR the bands at 1003 and 581 $cm^{-1}$ show a very similar intensity, while that at 886 $cm^{-1}$ is only some 20% of these two (Table 3). The noticeable intensity of this third band is due to the normal mode rotation between the 1 and the 9a upon deuteration[39,40] in such a way that the assignment order is reversed in pyrazine-$d_4$. These features of the RR spectrum between the ground state and the second exited singlet of the deuterated derivative have been satisfactorily reproduced by our procedure. Our scaled force field calculates the frequencies at 992, 883, and 593 $cm^{-1}$, respectively, for the three modes and the respective PED contribution being 100 $\nu_{ring}$, 80 $\delta$(CD) + 16 $\nu_{ring}$ and 85 $\delta_{ring}$ + 12 $\delta$(CD), for which they should be assigned in turn to the modes 1, 9a, and 6a. The rotation between the 9a and 1 modes upon deuteration can also be appreciated in the elements of the corresponding scrambling **S** matrix[41] constructed from the **L** matrices of the two isotopomers:

$$\mathbf{S} = \mathbf{L}^{-1}(d_4)\,\mathbf{L}(d_0) \tag{3}$$

This matrix points out that the fundamental at 992 $cm^{-1}$ should correspond to the 1 mode of the normal isotopomer ($\mathbf{S}_{992,1014} = 0.89$) and that registered at 883 $cm^{-1}$ to the 9a in turn ($\mathbf{S}_{883,1213} = 0.86$). On the other hand, the marked deviation of these elements in the **S** matrix confirm that the two fundamentals do mix due to the effect of deuteration. **ΔQ** values have been obtained by using the optimized geometries for the $S_2$ and $S_0$ states and the **L** matrix of the deuterated derivative (Table 6). As can be seen from inspection, the three significant values of 0.236, 0.128, and 0.376, respectively, are in good agreement with the experimental results.

Finally, Stock and Docke point out that the weak intensity of the 6a band in the preresonance spectrum with the $S_1$ state is due to destructive interference of the $S_1$ and $S_2$ Raman amplitudes, in spite of the fact that this band is the dominant progession-forming mode in the absorption spectrum.[42] This result is in agreement with the different sign showed in Table 6 for the **ΔQ** values of the 6a vibration in the $S_1$ and $S_2$ states.

**Final Remarks and Open Questions.** The analysis we propose is capable of encompassing some of the most notable features of the SERS-CT of pyrazine. Nevertheless, it can not explain the detailed behavior of the $A_g$ fundamental intensities with the electrode potential (see Table 4) nor the fact that bands assigned to non-totally-symmetric vibrations are recorded with

appreciable intensity. In relation to this point it could be thought that they are intensified via the EM mechanism which, without going into surface orientation considerations, would produce a general enhancement of all of the bands recorded in the pure liquid or solution Raman spectra. If this were true, the EM contribution to the SERS intensity corresponding to the 1 vibration could be obtained, for example, from the intensity of the 4 vibration, given that it should maintain a similar relationship to that in the spectrum of the pure liquid or the solution (see Table 3). If the intensity of the SERS band of the 4 mode at negative potentials was due just to the EM mechanism ($I_{rel}$ = 5 and 9 in the spectra of the pure liquid and SERS at −0.50 V, respectively), then the intensity of the 1 mode should be 180 which exceeds that observed. An alternative explanation could be that the non-totally-symmetric vibrations are active via other mechanisms different to the *A* term, in which case, analysis of SERS-CT results will be of a complexity similar to any other type of electronic spectroscopy.[43] In this respect, normal mode rotation between the $S_0$ and $D_0$ states would not appear to be important in the SERS of pyrazine given that the largest elements of the the Duschinsky matrix[26] for the $A_g$ fundamentals of pyrazine 2, 8a, 9a, 1, and 6a are 1.00, 0.99, 0.97, 0.95, and 1.00, respectively. This matrix has been computed by using the corresponding calculated **L** matrices (RHF and UHF/3-21G).

On the other hand, it is obvious that the enhancement of the $A_g$ modes should be favoured at more negative potentials if the charge transfer process is from the metal to the adsorbate. What is not so evident is a clear understanding of the behavior in the SERS reported by Moskovits et al.[9] with respect to the coverage. An alternative explanation to the surface reorientation would be to accept that the active sites for the CT mechanism are not the same as the active sites for adsorption. As these spectra have been obtained in conditions of low coverage, it seems reasonable to suggest that in an experiment carried out at submonolayer coverage the occupied sites would be the most active ones for adsorption. Upon increasing the coverage the incoming molecules would occupy the less active adsorption sites in which the CT mechanism would be more probable however. Another important factor not yet definitively understood is the effect of adsorption in the electronic properties of surface plasmons.[44]

Finally, the $\Delta\mathbf{Q}$ values obtained for $D_0-S_0$ are significantly greater than those obtained for $S_1-S_0$, in which case a stronger intensity of the combinations and overtones should be expected in the SERS-CT than for the RR. This prediction would not appear to be valid from looking at the spectra despite the fact that Creighton et al.[11] assign a good number of these vibrations in the SERS of pyridine at negative electrode potentials. There are two factors that could explain this discrepancy. In the first place, the amount of charge transferred in the excited state could perhaps be less than a complete electron. In this case the potential energy minimums of the $S_0$ and CT ($D_0$) states would not be as displaced as indicated by the ab initio results. Another important fact that would explain the weaker intensity of the overtones in SERS-CT compared with RR, is the experimentally proven fact that molecules at the surface have very efficient nonradiative decay mechanisms that drastically reduce the fluorescence in SERS.[45] Consequently, the mean lifetime of the excited state in SERS-CT would be remarkably shorter than in RR, which would imply that the nuclear relaxation in the first case would be less efficient despite the fact that the calculated $\Delta\mathbf{Q}$ values are actually greater.

## Conclusions

The hypothesis on which the preceding discussion has been based consists in supposing that the charge transfer in a SERS-CT experiment is from the metal to the adsorbate and amounts to a complete electron. In this way it has been possible to propose a procedure to predict the selective enhancement of certain bands by a simple comparison between the ab initio optimized geometries for the neutral molecule and the radical anion, and as a result presents a method for detecting charge-transfer processes in SERS. The results obtained are directly applicable to EELS spectroscopy under resonance conditions, while in SERS-CT the geometric changes are overestimated in the same way as was the transferred charge. Anyway, we think that it is a reasonable deduction that the 6a, 1, 9a, and the 8a fundamentals of pyrazine observed in the SERS on electrode are originated by a charge transfer process in an analogous way to that proposed for pyridine.

From the comparative study carried out, it is deduced that the calculation level does not significantly affect the predictions; RHF and UHF levels with 3-21G basis set are sufficient in order to give a satisfactory explanation of the experimental results. However, it is possible that this conclusion can not be extrapolated to molecules more complex than pyrazine. On the other hand, the numerical calculation of the normal mode displacements that connect the potential energy surface minimums yields much more relevant data than a direct comparison of the optimized geometries. The values of $\Delta\mathbf{Q}$ can be considered as semiquantitative selection rules applicable to the SERS active modes via a mechanism analogous to the *A* term in RR. The prediction capability has been satisfactorily checked with three published RR examples that involve the $S_1$ and the $S_2$ states, accounting for the different observed behavior of these spectra. We hope that from studies on less symmetric molecules it should be possible to extract more general conclusions.

**Acknowledgment.** The authors would like to express their gratitude to the DGICYT for the financial support for this work through Project PB93/0973/C02/01.

## References and Notes

(1) Fleischmann, M.; Hendra, P. J.; McQuillan, A. J. *Chem. Phys. Lett.* **1974**, *26*, 163.
(2) JeanMaire, D. L.; Van Duyne, R. P. *J. Electroanal. Chem.* **1977**, *84*, 1.
(3) Moskovits, M. *Rev. Mod. Phys.* **1985**, *57*, 783.
(4) Creighton, J. A. *The selection rules for surface-enhanced Raman spectroscopy*, in *Spectroscopy of Surfaces*; Clark R. J. H., Hester R. E., Eds.; Wiley: Chichester, 1988, and references therein.
(5) Otto, A.; Grabhorn, H.; Akeman, W. *J. Phys.: Condens. Matter* **1992**, *4*, 1143.
(6) Muniz-Miranda, M.; Neto, N.; Sbrana, G. *J. Phys. Chem.* **1988**, *92*, 954.
(7) Sinclair, T. J. *7th Int. Conf. Spectrosc. Raman* **1980**, 408.
(8) Erdheim, G. R.; Birke, R. L.; Lombardi, J. R. *Chem. Phys. Lett.* **1980**, *69*, 495.
(9) Moskovits, M.; DiLella, D. P.; Maynard, K. J. *Langmuir* **1988**, *4*, 67.
(10) Creighton, J. A.; Alvarez, M. S.; Weitz, D. A.; Garoff, S.; Kim, M. W. *J. Phys. Chem.* **1983**, *87*, 4793.
(11) Creighton, J. A. *Surf. Sci.* **1986**, *173*, 665.
(12) Gadzuk, J. W. *Annu. Rev. Phys. Chem.* **1988**, *39*, 395.
(13) Gadzuk, J. W. *J. Chem. Phys.* **1983**, *79*, 3982.
(14) Nenner, I.; Schulz, G. J. *J. Chem. Phys.* **1975**, *62*, 1747.
(15) Wong, S. F.; Schulz, G. J. *Phys. Rev. Lett.* **1975**, *35*, 1429.
(16) Otto, A. In *Light Scattering in Solid IV*. Topics in Applied Physics; Cardona, M.. Güntherodt, G., Eds.; Springer: Berlin, 1984; Vol. 54.
(17) Moskovits,M.; DiLella, D. P. *J. Chem. Phys.* **1980**, *73*, 6068.
(18) Strictly speaking, the radical anion is a different chemical species to the neutral molecule, but it can be considered in SERS as an excited electronic state of the metal−adsorbate system.
(19) Gallup, G. A. *J. Chem. Phys.* **1993**, *99*, 827.

(20) Clark, R. J. H.; Dines, T. J. *Angew. Chem., Int. Ed. Engl.* **1986**, *25*, 131.

(21) Strommen, D. P.; Nakamoto, K. *J. Chem. Educ.* **1977**, *54*, 474. Hirakawa, A. Y.; Tsuboi, M. *Science* **1975**, *188*, 359.

(22) Frisch, M. J.; Head-Gordon, M.; Trucks, G. W.; Foresman, J. B.; Schlegel, H. B.; Raghavachari, K.; Robb, M.; Binkley, J. S.; Gonzalez, C.; Defrees, D. J.; Fox, D.J.; Whiteside, R. A.; Seeger, R.; Melius, C. F.; Baker, J.; Martín, R. L.; Kahn, L. R.; Stewart, J. J. P.; Topiol, X.; Pople, J. A. *GAUSSIAN 90*, revision H; Gaussian, Inc.: Pittsburgh, PA, 1990.

(23) Hinde, A. L.; Poppinger, D.; Radom, L. *J. Am. Chem. Soc.* **1978**, *100*, 4681.

(24) Liu. R; Zhou, X. *J. Phys. Chem.* **1993**, *97*, 9613.

(25) Pulay, P; Hamilton, T. P. *J. Chem. Phys.* **1988**, *88*, 4926. Bofill, J. M.; Pulay, P. *J. Chem. Phys.* **1989**, *90*, 3637.

(26) Orlandi, G.; Zerbetto, F.; Zgierski, M. Z. *Chem. Rev.* **1991**, *91*, 867.

(27) Woywod, C.; Domcke, W.; Sobolewski, A. L.; Werner, H. *J. Chem. Phys.* **1994**, *100*, 1400.

(28) Arenas, J. F.; Lopez-Navarrete, J. T.; Otero, J. C.; Marcos, J. I.; Cardenete, A. *J. Chem. Soc., Faraday Trans. 2* **1985**, *81*, 405

(29) Arenas, J. F.; Lopez-Navarrete, J. T.; Marcos, J. I.; Otero, J. C. *Spectrochim. Acta* **1986**, *42A*, 1343.

(30) Varsányi, G. *Vibrational spectra of benzene derivatives*; Academic Press: New York, 1969.

(31) Arenas, J. F.; López Tocón, I.; Otero, J. C.; Marcos, J. I. *J. Phys. Chem.* **1995**, *99*, 11392.

(32) Pulay, P.; Fogarasi, G.; Pang, F.; Boggs, J. E. *J. Am. Chem. Soc.* **1979**, *101*, 2550.

(33) McIntosh, D. F.; Peterson, M. R. General Vibrational Analysis System, QCPE 576, 1989.

(34) Pulay, P.; Fogarasi, G.; Boggs, J. E. *J. Chem. Phys.* **1981**, *74*, 3999.

(35) Wiberg, K. B. *J. Mol. Struct.* **1990**, *244*, 61.

(36) Schmeisser, D.; Demuth, J. E.; Avouris, Ph. *Chem. Phys. Lett.* **1982**, *87*, 324.

(37) Yamada, H.; Toba, K.; Nakao, Y. *J. Electron Spectrosc. Relat. Phenom.* **1987**, *45*, 113. Yamada, H.; Nagaka, H.; Toba, K.; Nakao Y. *Surf. Sci.* **1987**, *182*, 269.

(38) Avouris, Ph.; Demuth, J. E. *J. Chem. Phys.* **1981**, *75*, 4783.

(39) Suzuka, I.; Udagawa, Y.; Ito, M. *Chem. Phys. Lett.* **1979**, *64*, 333.

(40) Simmons, J. C.; Innes, K. K.; Begun, G. M. *J. Mol. Spectrosc.* **1964**, *14*, 190.

(41) Rava, R. P.; Goodman, L. *J. Phys. Chem.* **1982**, *86*, 480.

(42) Stock, G.; Domcke, W. *J. Chem. Phys.* **1990**, *93*, 5496.

(43) While in the SERS of pyridine or pyrazine the strongest bands correspond to totally symmetric vibrations, the main features of the SERS of *p*-aminothiophenol have recently been analyzed via the Herzberg−Teller effect (*B* term): Osawa, M.; Matsuda, N.; Yoshii, K.; Uchida, I. *J. Phys. Chem.* **1994**, *98*, 12702.

(44) Henglein, A. *J. Phys. Chem.* **1993**, *97*, 5457.

(45) Pettinger, B.; Gerolymatou, A. *Bunsen-Ges. Ber. Phys. Chem.* **1984**, *88*, 359.

JP952240K